

Solubility of water ice in metallic hydrogen: consequences for core erosion in gas giant planets

H. F. Wilson

Department of Earth and Planetary Science, University of California, Berkeley, CA 94720, USA.

and

B. Militzer

Departments of Earth and Planetary Science and of Astronomy, University of California, Berkeley, CA 94720, USA.

ABSTRACT

Using *ab initio* simulations we investigate whether water ice is stable in the cores of giant planets, or whether it dissolves into the layer of metallic hydrogen above. By Gibbs free energy calculations we find that for pressures between 10 and 40 Mbar the ice-hydrogen interface is thermodynamically unstable at temperatures above approximately 3000 K, far below the temperature of the core-mantle boundaries in Jupiter and Saturn. This implies that the dissolution of core material into the fluid layers of giant planets is thermodynamically favoured, and that further modelling of the extent of core erosion is warranted.

Subject headings: planets and satellites: Jupiter, planets and satellites: Saturn, molecular processes, convection

1. Introduction

According to core accretion models (Mizuno et al. 1978), giant gas planets such as Jupiter and Saturn formed via the accumulation of a proto-core of rock and ice which gained solid material until it reached sufficient size to begin accreting the gaseous component of the protosolar nebula. The existence of solid ice in the outer solar system promotes the rapid growth of the more massive proto-cores allowing the accretion of large quantities of gas necessary for Jupiter-sized planets. Giant planets thus have a dense core of rock and ice surrounded by a H-He envelope. It is not known, however, whether the initial dense core remains stable following the accretion of the H-He outer layer or whether the core erodes into the fluid hydrogen-rich layers above (Stevenson 1982; Guillot et al. 2004).

The gravitational moments of Jupiter and Saturn, which have been measured by prior planetary missions and will be determined for Jupiter with

unprecedented accuracy by the upcoming Juno mission, may be used in combination with interior models (Militzer et al. 2008; Guillot et al. 2004; Hubbard 2005; Saumon and Guillot 2004; Nettelmann et al. 2008) to estimate the mass of the present-day core, but it is unclear whether these masses correspond to the primordial core mass. It has been suggested (Guillot et al. 2004; Saumon and Guillot 2004) that the present-day core mass of Jupiter may be too small to explain its formation by core accretion within the relatively short lifetime of the protosolar nebula (Pollack et al. 1996), although a more recent Jupiter model (Militzer et al. 2008) predicted a larger core of 14–18 Earth masses which is consistent with core accretion. Furthermore, direct measurements of Jupiter’s atmosphere suggest a significant enhancement in the concentration of heavy ($Z > 3$) elements (Niemann et al. 1996), but it is unknown to what extent this should be attributed to a large flux of late-arriving planetesimals versus the up-

welling of core material. Determining the extent of core erosion is thus a major priority for understanding the interiors of giant planets and the process by which they were formed.

In this work we focus on water ice, presumed to be a major constituent of the core, and consider the question of whether it has significant solubility in fluid metallic hydrogen at conditions corresponding to the core-mantle boundaries of giant gas planets. Water ice is the most prevalent of the planetary ices (water, methane and ammonia) which may be assumed to make up the outermost layers of a differentiated rock-ice core (Hubbard 1981). At the conditions of temperature and pressure prevalent at giant planet cores, water ice is predicted (Cavazzoni et al. 1999; French et al. 2009) to be in either in a fully atomic fluid phase in which oxygen and hydrogen migrate freely and independently, or in a superionic phase in which oxygen atoms vibrate around defined lattice sites while hydrogen atoms migrate freely. Assuming the existence of a core-mantle boundary at which water ice and the fluid H-He phase are in direct contact, the relevant question is the extent to which the system may lower its Gibbs free energy by the redistribution of the atoms of the ice phase into the fluid hydrogen. The extreme pressure and temperature conditions prevalent at giant planet core-mantle boundaries (8000–12000K and 8–18 Mbar for Saturn, 18000–21000K and 35–45 Mbar for Jupiter) are not yet obtainable in the laboratory, thus *ab initio* simulations provide the best available guide to determining the extent of core solubility.

2. Theory and Methodology

We used density functional molecular dynamics (DFT-MD) calculations and coupling constant integration (CCI) techniques to compute the Gibbs free energy of solvation, ΔG_{sol} , of H_2O in fluid metallic hydrogen, i.e. the change in Gibbs free energy when an H_2O molecule is removed from the pure ice phase and dissolved in H. The free energy of solubility is computed from the free energies of three systems: pure ice, pure fluid H, and a mixed system in which the atoms of one water molecule are dissolved in n atoms of hydrogen,

$$\Delta G_{sol} = G(\text{OH}_{n+2}) - [G(\text{H}_2\text{O}) + G(\text{H}_n)] \quad (1)$$

where $G(\text{H}_2\text{O})$ is the energy per H_2O stoichiometric unit of the ice phase, and $G(\text{H}_n)$ is obtained from an appropriately-scaled simulation of 128 H atoms. This quantity becomes more negative as solubility increases. A ΔG_{sol} of zero implies a saturation concentration of exactly one H_2O to n H. In order to span the range of likely conditions for the core-mantle boundary of Jupiter and Saturn, we considered pressures of 10, 20 and 40 Mbar, at a range of temperatures from 2000 to 20000 K.

Computation of free energies from MD simulations is difficult since the entropy term is not directly accessible. Here we use a two-step CCI approach as previously applied by several authors (Alfè et al. 1999; Morales et al. 2009; Wilson and Militzer 2010) to compute free energies. The CCI method provides a general scheme for computing ΔF between systems governed by potential energy functions U_1 and U_2 . We construct an artificial system U_λ whose forces are derived from a linear combination of the potential energies of the two systems $U_\lambda = (1 - \lambda)U_1 + \lambda U_2$. The difference in Helmholtz free energy between the two systems is then

$$\Delta F = \int_0^1 \langle U_2 - U_1 \rangle_\lambda d\lambda, \quad (2)$$

where the average is taken over the trajectories governed by the potential U_λ . We perform two CCIs for each G calculation: first from the DFT-MD system to a system governed by a classical pair potential which we fit to the DFT dynamics of the system via a force-matching approach (Izvekov et al. 2004), and then from the classical system to a reference system whose free energy is known analytically.

2.1. Material phases

The material phases in question must be established prior to the Gibbs free energy calculations. At the pressure and temperature conditions of interest, hydrogen is a metallic fluid of H atoms in which molecular bonds are not stable. Water dissolved within hydrogen likewise is non-molecular, with a free O atom in an atomic H fluid. For water ice, the phase diagram at giant planet core pressures is divided into three regimes (Cavazzoni et al. 1999; Goldman

et al. 2005; Mattsson and Desjarlais 2006; French et al. 2009): a low-temperature (< 2000 K) crystalline regime, an intermediate superionic regime in which oxygen atoms vibrate around fixed lattice sites while hydrogen atoms migrate freely, and a higher-temperature fully fluid regime in which both hydrogen and oxygen atoms are mobile. The transition between the crystalline and superionic regimes has not yet been studied in detail at high pressures but our simulations find that it occurs below 2000 K. The transition from superionic to fully fluid is found to occur in simulation at temperatures ranging from 8000 K for 10 Mbar and 13000 K for 50 Mbar (French et al. 2009). Consequently our study includes the superionic and fully fluid ice phases.

Previous studies of superionic ice (Cavazzoni et al. 1999; French et al. 2009) have used an *bcc* arrangement of atoms for the oxygen sublattice. We found that such a lattice was stable at all points studied in the superionic regime except for 10 Mbar at 2000 and 3000 K. At these conditions we found that the oxygen sublattice was stable in the *Pbca* geometry which we recently reported to be the most stable zero-temperature structure for ice at 10 Mbar (Militzer and Wilson 2010). At 10 Mbar and 5000 K, superionic ice with a *bcc* sublattice was stable but the *Pbca* was not. The *bcc* oxygen sublattice was found to be stable for 20 and 40 Mbar pressures at all temperatures studied in the superionic regime. Attempts to perform a superionic simulation in the *Cmcm* geometry reported by Militzer and Wilson (2010) to be the stable zero-temperature structure at these pressures resulted in an unstable system with a large anisotropic strain. We thus used a *bcc* oxygen sublattice for all superionic ice simulations, except the 2000 K and 3000 K simulations at 10 Mbar which used the oxygen sublattice from the *Pbca* phase, as indicated in Figure 1. While we cannot yet exclude the possibility of the existence of yet another superionic ice structure, we note that the differences between different ice phase energies are found to be on the order 0.1 eV per H_2O , and thus will not significantly affect our results about the stability of ice in giant planet cores.

2.2. Computation of Gibbs free energies

Our goal in this paper is to study the solubility of water ice in fluid hydrogen. Due to considera-

tions arising from the entropy of mixing, the solubility of one material in another is never zero, however solubility at trace quantities is not sufficient for core erosion. In particular, we wish to know whether solubility is thermodynamically favored at concentrations significantly greater than the background concentration of oxygen in the fluid envelope of Jupiter or Saturn – this is equal to approximately one O atom to 1000 H atoms if we assume solar concentrations for the Jovian envelope and approximately one part in 300 if we assume a threefold enrichment for oxygen as observed for most other heavy elements (Mahaffy et al. 1998). We begin by computing the Gibbs free energies of solubility for dissolving H_2O in pure H at one part in 125, and generalize later.

The coupling constant integration approach requires, as an integration end point, a reference system whose free energy may be computed analytically. It is important to ensure that the system does not undergo a phase change along the integration pathway since this may cause numerical difficulties in the integration. For the fluid systems, being pure hydrogen, hydrogen with oxygen, and ice at temperatures above the superionic-to-fluid transition, we used an ideal atomic gas as the reference system (Alfè et al. 1999; Morales et al. 2009; Wilson and Militzer 2010). For superionic ice, we use as a reference system a combination of an ideal gas system for the hydrogen atoms with an Einstein crystal of oxygen atoms each oxygen tethered to its ideal lattice site with a harmonic potential of spring constant $30 \text{ eV}/\text{\AA}^2$.

The DFT-MD simulations in this work used the Vienna Ab Initio Simulation Package (VASP) (Kresse and Furthmüller 1996) with pseudopotentials of the projector augmented wave type (Blöchl 1994) and the exchange-correlation functional of Perdew et al. (1996). The pseudopotentials used had a core radius of 0.8 Å for hydrogen and 1.1 Å for oxygen. Wavefunctions were expanded in a basis set of plane waves with a 900 eV cutoff and the Brillouin Zone was sampled with $2 \times 2 \times 2$ *k*-points. The electronic temperature effects were taken into account via Fermi-Dirac smearing. A new set of force-matched potentials was fitted for each pressure-temperature conditions for each stoichiometry. All MD simulations used a 0.2 fs timestep. In the classical potential under superionic conditions, an additional harmonic potential

term was added to ensure that oxygen atoms remained in the appropriate lattice sites, however, we found that in most cases the fitted pair potential alone was sufficient to stabilize the superionic state.

The first step of the free energy calculations was the determination of the appropriate supercell volumes for each system for each set of pressure and temperature conditions. This was accomplished via constant-pressure MD simulations (Hernández 2001; Hernández et al. 2010) with a duration of 1.6 ps (0.6 ps for ice). DFT-MD trajectories were then computed in a fixed cell geometry in order to fit classical potentials. A run of 0.4 ps was found to be sufficient for fitting suitable potential. We then performed molecular dynamics runs 600 fs long (400 fs for ice) at five λ values to integrate between the DFT and classical systems. Finally, we performed classical Metropolis Monte Carlo at 24 λ values to integrate from the classical to the reference system.

3. Simulation results

Table I lists the total Gibbs free energies for each simulated system (H_{128} , OH_{127} and ice) for each set of temperature and pressure conditions. Ice was confirmed to remain superionic except at the 20 Mbar/12000 K and 40 Mbar/20000 K conditions where it was fully fluid. The error bars on the computed G values are dominated primarily by the uncertainty in the computed volume at the desired pressure, and secondarily by uncertainty in the $\langle U_{DFT} - U_{classical} \rangle_{\lambda}$ term in the coupling constant integration. These free energies are combined using Equation 1 to give ΔG_{sol} representing the free energy change associated with removing an H_2O from the ice phase and dissolving it in the hydrogen fluid at a concentration of molecule per 125 solute H atoms. ΔG_{sol} increases strongly with temperature, but shows only a weak dependence on pressure within the 10–40 Mbar range under consideration. The ΔG values were found to be well converged with respect to wavefunction cutoff, k-point sampling to within the available error bars. The effect of the electronic entropy term on ΔG_{sol} was found to be less than 0.1 eV in all cases. From a linear interpolation through the adjacent data points we estimated the temperature at which ΔG_{sol} passes through zero as 2400 K \pm

200 K at 40 Mbar, 2800 K \pm 200 K at 20 Mbar, and 3400 K \pm 600 K at 10 Mbar. As shown in Figure 1, this is clearly far lower than any reasonable estimate for the core-mantle boundaries for either Jupiter or Saturn. The onset of high solubility occurs within the portion of the phase diagram where ice is superionic, and does not coincide with either the superionic-to-fluid transition or the crystalline-to-superionic transition in ice.

The total ΔG of solubility may be broken down into three components: a ΔU term from the potential energy, a $P\Delta V$ term from the volume difference, and a $-T\Delta S$ entropic term. Figure 2 shows this breakdown as a function of temperature for 20 Mbar. The breakdown for other pressures looks similar. The ΔU term, representing the difference in chemical binding energy, provides approximately a 2 eV per molecule preference for ice formation at all temperatures where ice is superionic, but a much smaller preference for the 12000 K case where ice is fluid. The PV term is indistinguishable from zero within the error bars, suggesting that this is not a pressure-driven transition, in contrast to recent results on the partitioning of noble gases between hydrogen and helium in giant planet interiors in which volume effects were found to be the dominant term (Wilson and Militzer 2010). The $-T\Delta S$ term dominates the temperature-dependent behavior, underlining that ice dissolution is indeed an entropy-driven process.

Given the Gibbs free energy of solubility for the insertion of one H_2O into 125 H atoms we can determine an approximate Gibbs free energy of solubility at other concentrations, by neglecting the contribution of the oxygen-oxygen interaction and including only the entropic term arising from the mixing. Under these approximations, we obtain the expression

$$\begin{aligned} \frac{\Delta G_{sol}[m] - \Delta G_{sol}[n]}{k_B T} &= (m+2) \log \left(\frac{(m+2)V_H + V_O}{(m+2)V_H} \right) \\ &- (n+2) \log \left(\frac{(n+2)V_H + V_O}{(n+2)V_H} \right) \\ &- \log \left(\frac{m+2}{n+2} \right), \end{aligned} \quad (3)$$

where V_H and V_O are the effective volumes of each H and O atom in the fluid. This approxi-

mation becomes invalid as the oxygen-oxygen interaction term in the fluid oxygen phase becomes significant, however for our purposes it is sufficient to know that the saturation concentration is significantly higher than the background concentration. If a saturation concentration of oxygen in hydrogen does indeed exist then this may be expected to have a retarding effect on the erosion of the core.

We must also consider possibility that hydrogen and oxygen could dissolve separately from the H₂O mixture, leaving behind a condensed phase with stoichiometry other than H₂O. We tested two cases explicitly, computing the free energies of pure oxygen and one-to-one HO phases at the Jupiter-like 40 Mbar, 20,000 K set of conditions. Both O and HO were found to be in a fully fluid state at these temperature/pressure conditions. We found that HO had a free energy of solubility of -11.2 eV per oxygen, while pure oxygen had -22.8 eV per oxygen. Comparing to the -8.9 eV per oxygen solubility of H₂O, this suggests oxygen-rich condensed phases are less thermodynamically stable than the H₂O phase, and certainly far less favourable than dissolution of the dense phase into metallic hydrogen. We have also neglected the possibility of hydrogen-enriched dense phases such as H₃O. While it possible such phases may be somewhat energetically preferred to H₂O, it is extremely unlikely that the preference will be strong compared to the 8 – 12 eV per O unit preference for solubility.

In Figure 3 we plot the estimated ΔG_{sol} as a function of concentration for various computed temperatures at a pressure of 40 Mbar. A negative value of ΔG_{sol} means that it is thermodynamically favorable to dissolve further ice into the hydrogen phase at a given hydrogen-phase ice concentration, and the point at which ΔG_{sol} is zero is the saturation concentration. For 2000 K and 3000 K the saturation concentrations are estimated to be on the order of 1:500 and 1:20 respectively, while for higher temperatures the saturation concentration is much higher. Given that we neglect O–O interactions in the fluid hydrogen phase, it is difficult to precisely determine the saturation concentrations for higher temperatures. However, we may safely say that the saturation concentration for temperatures in excess of 3000 K is very much greater than the background oxygen concentration, and hence that solubility of ice into hydrogen at the core-

mantle boundaries of Jupiter and Saturn is expected to be strongly thermodynamically favored.

4. Discussion

The consequences of core erosion for planetary evolution models have been previously considered by Stevenson (1982) and later Guillot et al. (2004). The effects of core erosion can potentially be detected either by orbital probes such as Juno or by atmospheric entry probes, since the redistribution of core material throughout the planet will manifest itself both by a smaller core (detectable from gravitational moments) and a higher concentration of heavy elements in the atmosphere than would be expected in a planet without core erosion. Once core material has dissolved into the metallic H layers, the rate at which core material can be redistributed throughout the planet is expected to be limited by double diffusive convection (Turner 1974; Huppert and Turner 1981). Since the higher density due to compositional gradients of the lower material interferes with the convection process, convection may be slowed significantly. Guillot et al. (2004) modelled the effect of core erosion under the assumptions of fully soluble 30 Mbar core in each planet. Under their assumptions up to 19 Earth masses could have been redistributed from Jupiter’s core but only 2 Earth masses from Saturn’s, the difference being Jupiter’s higher temperatures. While this prediction is subject to significant uncertainty in many aspects of the model, it does suggest that a redistribution of a significant fraction of the initial protocore is possible, at least in Jupiter. Further refinement of models for the upconvection of core material and its observable consequences may be fruitful. The effect of core erosion on the heat transport and mass distribution properties of Jupiter and Saturn should also be taken into account in future static models of these planets’ interiors.

These calculations can be expanded in several ways. We have neglected the presence of helium in the hydrogen-rich mantle, however due to the large magnitude of ΔG_{sol} and the chemical inertness of helium we do not expect the presence of helium in the mantle to significantly affect the solubility behavior. We have explicitly made the assumption that ice and hydrogen are in direct

contact, an assumption which might fail in one of two ways. If hydrogen and helium are immiscible at the base of the atmosphere then the core may make direct contact with a helium-rich layer. This, however, is unlikely in the context of the calculations of Morales et al. (2009) who predict hydrogen-helium immiscibility only far away from the cores of Jupiter and Saturn. The other possibility is that the ice layers of the core may be gravitationally differentiated, leaving ice beneath layers of the less dense planetary ices methane and ammonia. Since the bonding in these is similar to that in water ice one could assume that they show a similar solubility behavior, but this analysis is the subject of future work.

We have also considered only the structure of the present-day planet. As suggested by Iaroslavitz and Podolak (2006), a proper consideration of core solubility must also include solubility during the formation process, as dissolution of the icy parts of the core into the accreting hydrogen during the formation may result in the amount of ice on the core itself being small by the time the planet reaches its final size. A treatment of the formation processes for Jupiter and Saturn using ice solubilities derived from *ab initio* calculations may be valuable.

Our calculations strongly suggest that icy core components are highly soluble in the fluid mantle under the conditions prevalent at the core-mantle boundaries of Jupiter and Saturn. Since many recently-discovered exoplanets are more massive and hence internally hotter than Jupiter, it can be expected that any initial icy cores in these exoplanets will also dissolve. The presence of core erosion may allow models predicting a small present-day Jovian core to be made consistent with the large initial core required by core erosion, however models of the interior mass distribution of the planet will need to be revised to take the inhomogeneous composition of the lower layers implied by convection-limited core redistribution into account. Improved models which include core redistribution processes, combined with the data from the Juno probe, may assist in understanding the history and present structure of Jupiter and other planets in our own and in other solar systems.

This work was supported by NASA and NSF. Computational resources were supplied in part by

TAC, NCCS and NERSC. We thank D. Stevenson for discussions.

REFERENCES

- Alfè, D., Gilland, M. J., Price, G. D., 1999. The melting curve of iron at the pressures of the Earth's core from *ab initio* calculations. *Nature* 401, 462.
- Blöchl, P. E., 1994. Projector augmented-wave method. *Phys. Rev. B* 50, 17953.
- Cavazzoni, C., Chiarotti, G. L., Scandolo, S., Tosatti, E., Bernasconi, M., Parrinello, M., 1999. Superionic and metallic states of water and ammonia at giant planet conditions. *Science* 283, 44.
- French, M., Mattson, T. R., Nettelmann, N., Redmer, R., 2009. Equation of state and phase diagram of water at ultrahigh pressures as in planetary interiors. *Phys. Rev. B* 79, 054107.
- Goldman, N., Fried, L. E., Kao, I.-F. W., Mundy, C. J., 2005. Bonding in the superionic phase of water. *Phys. Rev. Lett.* 94, 217801.
- Guillot, T., Stevenson, D. J., Hubbard, W. B., Saumon, D., 2004. The interior of Jupiter. pp. 35–57.
- Hernández, E., 2001. Metric-tensor flexible-cell algorithm for isothermal-isobaric molecular dynamics simulations. *J. Chem. Phys.* 115, 10282.
- Hernández, E. R., Rodriguez-Prieto, A., Bergara, A., Alfè, D., 2010. First-principles simulations of lithium melting: Stability of bcc phase close to melting. *Phys. Rev. Lett.* 104, 185701.
- Hubbard, W. B., 1981. Interiors of the giant planets. *Science* 214, 145.
- Hubbard, W. B., 2005. Hydrogen EOS at megabar pressures and the search for Jupiter's core. *Astrophysics and Space Science* 298, 129.
- Huppert, H. E., Turner, J. S., 1981. Double-diffusive convection. *J. Fluid Mech* 106, 299.
- Iaroslavitz, E., Podolak, M., 2006. Atmospheric mass deposition by captured planetesimals. *Icarus* 187, 600.
- Izvekov, S., Parrinello, M., Burnham, C. J., Voth, G. A., 2004. Effective force fields for condensed phase systems from *ab initio* molecular dynamics simulation: A new method for force-matching. *J. Chem. Phys.* 120, 10896.
- Kresse, G., Furthmüller, J., 1996. Efficient iterative schemes for *ab initio* total-energy calculations using a plane-wave basis set. *Phys. Rev. B* 54, 11169.
- Mahaffy, P. R., Niemann, H. B., Alpert, A., Atreya, S. K., Donahue, T. M., Owen, T. C., 1998. Heavy noble gases in the atmosphere of Jupiter. *Bull. Am. Astron. Soc.* 30, 1066.
- Mattsson, T. R., Desjarlais, M. P., 2006. Phase diagram and electrical conductivity of high energy-density water from density functional theory. *Phys. Rev. Lett.* 97, 017801.
- Militzer, B., Hubbard, W. B., Vorberger, J., Tamblyn, I., Bonev, S. A., 2008. A massive core in Jupiter predicted from first-principles simulations. *ApJ* 688, L45.
- Militzer, B., Wilson, H. F., 2010. New phases of water ice predicted at megabar pressures. *Phys. Rev. Lett.* 105, 195701.
- Mizuno, H., Nakazawa, K., Hayashi, C., 1978. Instability of a gaseous envelope surrounding a planetary core and formation of giant planets. *Prog. Theor. Phys.* 60, 699.
- Morales, M. A., Schwegler, E., Ceperley, D., Pierleoni, C., Hamel, S., Caspersen, K., 2009. Phase separation in hydrogen-helium mixtures at Mbar pressures. *PNAS* 106, 1324.
- Niemann, H. B., Atreya, S. K., Carignan, G. R., Donahue, T. M., Haberman, J. A., Harpold, D. N., Hartle, R. E., Hunten, D. M., Kasprzak, W. T., Mahaffy, P. R., Owen, T. C., Spencer, N. W., Way, S. H., 1996. The Galileo probe mass spectrometer: Composition of Jupiter's atmosphere. *Science* 272, 846.
- Nettelmann, N., Holst, B., Kietzmann, A., French, M., Redmer, R., Blaschke, D., 2008. *Ab initio* Equation of State data for hydrogen, helium, and water and the internal structure of Jupiter. *Astrophys. J.* 683, 1217.
- Perdew, J. P., Burke, K., Ernzerhof, M., 1996. Generalized Gradient Approximation made simple. *Phys. Rev. Lett.* 77, 3865.

- Pollack, J. B., Hubickyj, O., Bodenheimer, P., Lissauer, J., Podolak, M., Greenzweig, Y., 1996. Formation of the giant planets by concurrent accretion of solids and gas. *Icarus* 124, 62.
- Saumon, D., Guillot, T., 2004. Shock compression of deuterium and the interiors of Jupiter and Saturn. *Astrop. J* 609, 1170.
- Stevenson, D. J., 1982. Formation of the giant planets. *Planet. Space. Sci* 30, 755.
- Turner, J. S., 1974. Double-diffusive phenomena. *Ann. Rev. Fluid. Mech.* 6, 37.
- Wilson, H. F., Militzer, B., 2010. Sequestration of noble gases in giant planet interiors. *Phys. Rev. Lett.* 104, 121101.

P (Mbar)	T (K)	$G(\text{H}_{128})$ (eV)	$G(\text{H}_{127}\text{O})$ (eV)	$G(\text{Ice})$ (eV)	ΔG_{sol} (eV)
10	2000	716.1(5)	728.4(4)	1800.2(22)*	0.97(62)
10	3000	672.2(3)	683.9(4)	1731.4(22)*	0.35(52)
10	5000	561.8(3)	571.7(3)	1311.5(11)	-1.10(50)
20	2000	1308.3(1)	1332.8(2)	2945.3(10)	0.61(24)
20	3000	1271.2(1)	1295.1(2)	2895.8(9)	0.11(22)
20	5000	1173.0(3)	1195.3(2)	2795.2(15)	-1.91(37)
20	8000	989.7(7)	1009.9(4)	2536.5(15)	-3.57(80)
20	12000	705.9(10)	722.5(6)	2049.8(26) [†]	-4.8(12)
40	2000	2161.5(1)	2205.5(1)	5102.2(10)	0.18(14)
40	3000	2131.3(1)	2174.8(1)	5062.6(10)	-0.25(17)
40	5000	2046.0(3)	2087.9(2)	4943.0(13)	-1.69(30)
40	8000	1880.8(4)	1920.3(2)	4701.3(13)	-3.47(43)
40	20000	1011.6(17)	1041.1(14)	3350.6(30) [†]	-8.9(22)

Table 1: Gibbs free energies per simulation cell of fluid hydrogen, fluid hydrogen with oxygen, and ice at each temperature/pressure combination, along with the energy of solvation ΔG_{sol} per H_2O molecule. Ice systems marked with a star have $\text{H}_{128}\text{O}_{64}$ stoichiometry and an oxygen structure from the *Pbca* phase while other ice systems have $\text{H}_{108}\text{O}_{54}$ and a *bcc* oxygen sublattice. Ice systems marked with a dagger are fully fluid, while others are superionic.

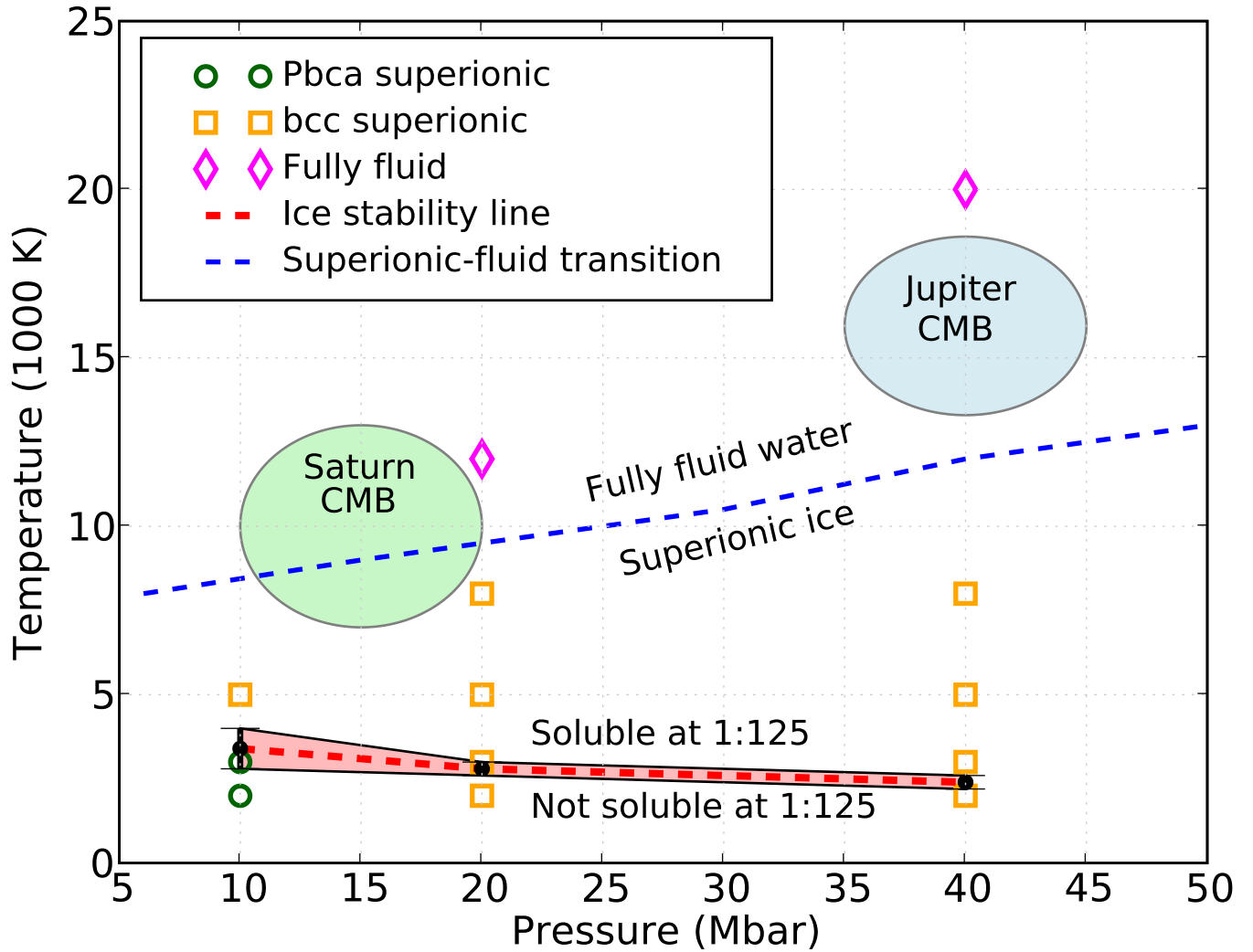


Fig. 1.— (Color online) Computed location of the temperature at which saturation is reached at 1:125, as a function of pressure between 10 and 40 Mbar, with the shaded area corresponding to error bars, in relation to the approximate location of the superionic-to-fluid transition (French et al. 2009), and the approximate conditions corresponding to the core-mantle boundaries of Jupiter and Saturn. The points at which calculations have been undertaken are marked, with the shape and color of the symbols indicating phase of ice used in each calculation.

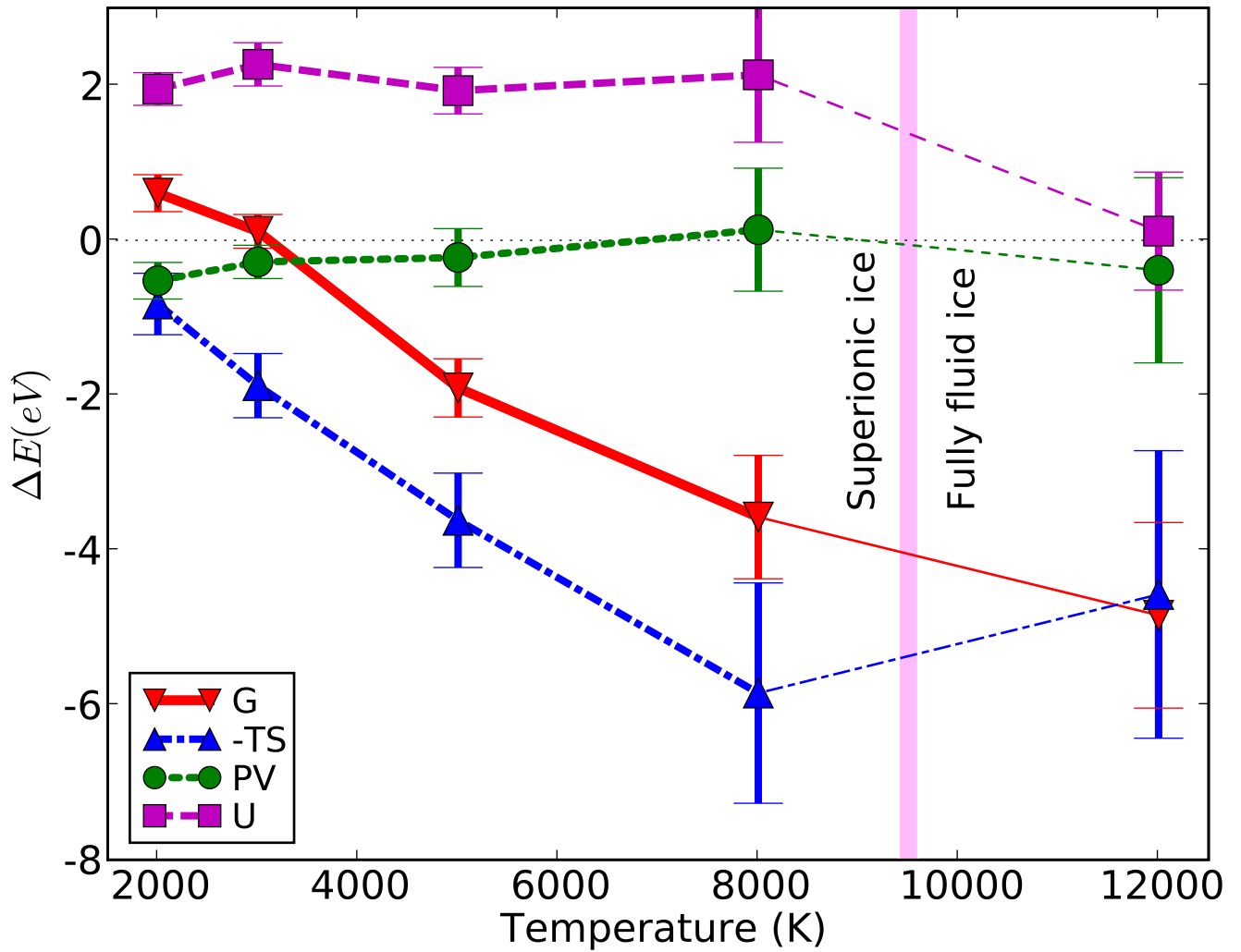


Fig. 2.— Breakdown of the computed ΔG_{sol} into contributions from the ΔU , $P\Delta V$, and $-T\Delta S$ terms, as a function of temperature, at a pressure of 20 Mbar.

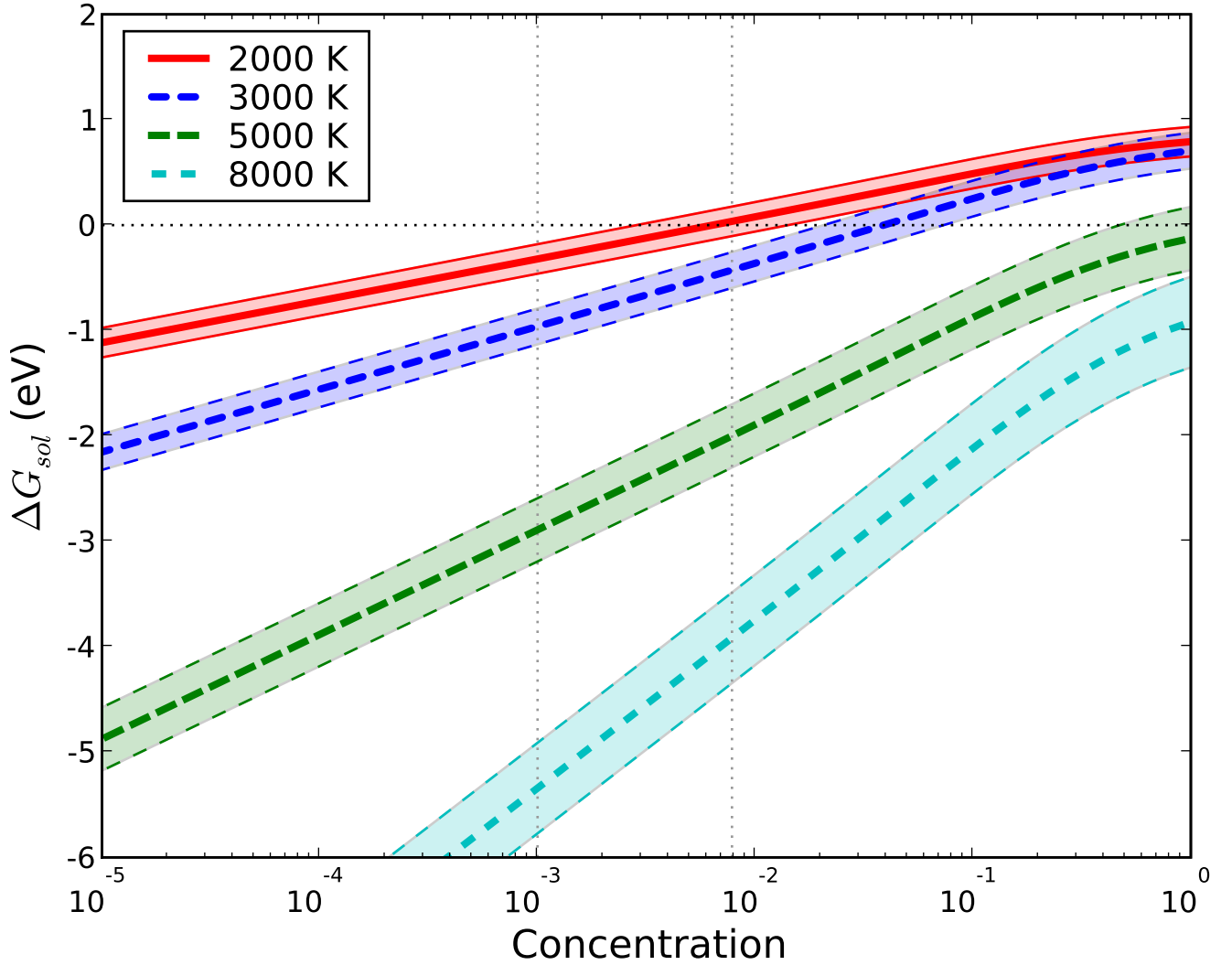


Fig. 3.— Estimated free energy of solubility ΔG_{sol} of ice in hydrogen as a function of oxygen concentration in the limit where oxygen atoms do not interact in the fluid phase, for various temperatures at a pressure of 40 Mbar. Shaded regions indicate error bars.